

Infrared absorption spectra from organic matter in the asteroid Ryugu samples: Some unique properties compared to unheated carbonaceous chondrites

Yoko KEBUKAWA ^{1*}, Eric QUIRICO², Emmanuel DARTOIS³, Hikaru YABUTA⁴,
Laure BEJACH⁵, Lydie BONAL², Alexandre DAZZI⁶, Ariane DENISET-BESSEAU⁶,
Jean DUPRAT ⁷, Cecile ENGRAND⁵, Jérémie MATHURIN ⁶, Jens BAROSCH ⁸,
George D. CODY ⁸, Bradley DE GREGORIO ⁹, Minako HASHIGUCHI¹⁰, Kanami KAMIDE⁴,
David KILCOYNE¹¹, Mutsumi KOMATSU ^{12,13}, Zita MARTINS¹⁴, Gilles MONTAGNAC¹⁵,
Smail MOSTEFAOUI⁷, Larry R. NITTLER ^{8,16}, Takuji OHIGASHI¹⁷, Taiga OKUMURA¹⁸,
Laurent REMUSAT⁷, Scott SANDFORD ¹⁹, Miho SHIGENAKA⁴, Rhonda STROUD^{9,16},
Hiroki SUGA²⁰, Yoshio TAKAHASHI¹⁸, Yasuo TAKEICHI²¹, Yusuke TAMENORI²⁰,
Maximilien VERDIER-PAOLETTI⁷, Daisuke WAKABAYASHI²¹, Shohei YAMASHITA²¹,
Hisayoshi YURIMOTO ²², Tomoki NAKAMURA²³, Takaaki NOGUCHI ²⁴, Ryuji OKAZAKI²⁵,
Hiroshi NARAOKA²⁵, Kanako SAKAMOTO²⁶, Shogo TACHIBANA ¹⁸, Toru YADA²⁶,
Masahiro NISHIMURA²⁶, Aiko NAKATO²⁶, Akiko MIYAZAKI²⁶, Kasumi YOGATA²⁶,
Masanao ABE²⁶, Tatsuaki OKADA²⁶, Tomohiro USUI²⁶, Makoto YOSHIKAWA²⁶, Takanao SAIKI²⁶,
Satoshi TANAKA²⁶, Fuyuto TERUI²⁷, Satoru NAKAZAWA²⁶, Sei-ichiro WATANABE¹⁰, and
Yuichi TSUDA²⁶

¹Department of Chemistry and Life Science, Yokohama National University, Yokohama, Japan

²CNRS, Institut de Planétologie et d'Astrophysique (IPAG), UMR 5274, Université Grenoble Alpes, Grenoble, France

³Institut des Sciences Moléculaires d'Orsay, Centre National de la Recherche Scientifique, Université Paris-Saclay, Orsay, France

⁴Department of Earth and Planetary Systems Science, Hiroshima University, Hiroshima, Japan

⁵Laboratoire de Physique des 2 Infinis Irène Joliot-Curie, Centre National de la Recherche Scientifique, Université Paris-Saclay, Orsay, France

⁶Institut Chimie Physique, Centre National de la Recherche Scientifique, Université Paris-Saclay, Orsay, France

⁷Institut de Mineralogie, Physique des Matériaux et Cosmochimie, Muséum National d'Histoire Naturelle, Centre National de la Recherche Scientifique, Sorbonne Université, Paris, France

⁸Earth and Planets Laboratory, Carnegie Institution for Science, Washington, DC, USA

⁹Materials Science and Technology Division, US Naval Research Laboratory, Washington, DC, USA

¹⁰Graduate School of Environmental Studies, Nagoya University, Nagoya, Japan

¹¹Advanced Light Source, Lawrence Berkeley National Laboratory, Berkeley, California, USA

¹²Center for University-Wide Education, Saitama Prefectural University, Saitama, Japan

¹³Department of Earth Sciences, Waseda University, Tokyo, Japan

¹⁴Centro de Química Estrutural, Institute of Molecular Sciences, Department of Chemical Engineering, Instituto Superior Técnico, Universidade de Lisboa, Lisbon, Portugal

¹⁵École normale supérieure de Lyon, University Lyon 1, Lyon, France

¹⁶School of Earth and Space Exploration, Arizona State University, Tempe, Arizona, USA

¹⁷Institute for Molecular Science, UVSOR Synchrotron Facility, Okazaki, Japan

¹⁸Department of Earth and Planetary Science, The University of Tokyo, Tokyo, Japan

¹⁹NASA Ames Research Center, Moffett Field, California, USA

²⁰Japan Synchrotron Radiation Research Institute, Hyogo, Japan

²¹Institute of Materials Structure Science, High Energy Accelerator Research Organization, Tsukuba, Japan

²²Department of Earth and Planetary Sciences, Hokkaido University, Sapporo, Japan

²³Department of Earth Science, Tohoku University, Sendai, Japan

²⁴Department of Earth and Planetary Sciences, Kyoto University, Kyoto, Japan

²⁵Department of Earth and Planetary Sciences, Kyushu University, Fukuoka, Japan

²⁶Institute of Space and Astronautical Science, Japan Aerospace Exploration Agency (JAXA), Sagami-hara, Japan

²⁷Kanagawa Institute of Technology, Atsugi, Japan

***Correspondence**

Yoko Kebukawa, Department of Chemistry and Life Science, Yokohama National University, 79-5 Tokiwadai, Hodogaya-ku, Yokohama 240-8501, Japan.

Email: kebukawa.y.aa@m.titech.ac.jp

(Received 21 April 2023; revision accepted 31 July 2023)

Abstract—The infrared spectral characteristics of organic-rich acid residues prepared from Ryugu samples returned by the JAXA Hayabusa2 mission generally match those from unheated carbonaceous chondrite meteorites, but the residues from Ryugu are richer in methyl and methylene functional groups and have higher CH_2/CH_3 ratios. Moreover, two distinct outlier carbonaceous phases are found; one with spectral characteristics of N-H functional groups, likely amides, and a second phase containing less nitrogen. Such infrared characteristics of Ryugu organic matter might indicate the pristine nature of the freshly collected samples and reflect the near-surface chemistry in the parent asteroid.

INTRODUCTION

Chondrite meteorites preserve information about primordial building blocks of the solar system. Particularly, carbonaceous chondrites (CCs) contain organic matter and hydrated minerals that provided prebiotic organic matter and water to the early Earth. However, many of the most well-studied meteorites have been exposed to terrestrial atmosphere and laboratory environments for a significant period of time, and thus, the possibilities of degradation and contamination must be considered (e.g., Martins et al., 2007). While it is impossible to completely eliminate the sources of terrestrial organic contamination on sample return missions from the parent body of meteorites, that is, the asteroids, organic matter is crucial to answer fundamental questions about the nature and diversity of the organic matter at the birth and evolution of our solar system (Chan et al., 2020). In this regard, direct sampling from asteroids is a desired opportunity to obtain primitive samples from C-type asteroids, including geological context. Surface samples from 162173 Ryugu, a C-type asteroid were successfully obtained by the Hayabusa2 mission and returned to the Earth on December 6, 2020. The first and second touchdown samples were separately stored in chambers A and chamber C, respectively, of the sample container. The second touchdown samples are expected to contain the ejecta from the subsurface exposed by an artificial impact prior to collection (Arakawa et al., 2020; Tachibana et al., 2022). Preliminary analysis of the Ryugu samples was conducted by the six Hayabusa2 initial analysis teams (IATs) from June 2021 to May 2022, after curation and initial description at the Japan Aerospace Exploration Agency (JAXA). The IATs revealed

the connection between Ryugu samples and CI chondrite meteorites, but Ryugu samples were more chemically pristine (Nakamura et al., 2023; Yokoyama et al., 2023). The organic macromolecule IAT was tasked with measuring organic functional group, elemental, and isotopic compositions of organic matter present in Ryugu particles and organic-rich acid residues extracted from Ryugu particles, to decipher the nature of the organic matter and its origin, parent body processing, and interaction with water and minerals (Yabuta et al., 2023).

Fourier transform infrared (FT-IR) spectroscopy is a nondestructive technique for detecting functional group chemistry and structures, which is suitable for both organic and inorganic compounds. To date, IR absorption spectra (in transmission mode) have been obtained from various chondrites (Beck et al., 2010, 2014; Bonal et al., 2013; Briani et al., 2013; Kebukawa et al., 2019; Osawa et al., 2005; Quirico et al., 2014, 2018) and other astromaterials, such as interplanetary dust particles (IDPs; Brunetto et al., 2011; Flynn et al., 2003; Keller et al., 2004; Matrajt et al., 2005), micrometeorites (Battandier et al., 2018; Dartois et al., 2013, 2018), and cometary dust particles (Sandford et al., 2006, 2010), as well as for organic residues from acid demineralization, so-called insoluble organic matter (IOM), from various chondrites (Alexander et al., 2014; Kebukawa et al., 2011; Orthous-Daunay et al., 2013; Quirico et al., 2014, 2018). These IR studies revealed parent body process affecting both organics and minerals—molecular structure changes such as loss of aliphatic structures and carbonyls due to hydrothermal alteration/thermal metamorphism (Alexander et al., 2014; Kebukawa et al., 2011; Orthous-Daunay et al., 2013; Quirico et al., 2014, 2018), and evolution of mineralogy such as level of hydration and Mg numbers of olivines (e.g., Beck et al., 2010, 2014), as well as comparison to spectroscopic observations of solar

[Correction added on 13 Sep 2023, after first online publication: The email address of the corresponding author was changed.]

system bodies and interstellar medium (e.g., Brunetto et al., 2011; Muñoz Caro & Dartois, 2009). Here, we report micro-FT-IR analysis of the acid residues from Ryugu samples to understand the nature of organic matter in Ryugu. Complementary results are also presented by Quirico et al. (under review), and the FT-IR results of untreated particles are presented by Dartois et al. (2023) (synchrotron and conventional FT-IR).

METHODS

Acid residues from A0106 and C0107 aggregates, collected at the first and second touchdown operations, respectively, were prepared by HF/HCl demineralization at Hiroshima University (Yabuta et al., 2023) after solvent extraction with hexane, dichloromethane, methanol, hot water, formic acid, and HCl, by the soluble organic molecule (SOM) IAT (Naraoka et al., 2023). An organic-free antigorite (a phyllosilicate mineral) blank was also subjected to HF/HCl demineralization at the same time. An acid residue from the C0002 grain, collected at the second touchdown site, was also prepared separately at Hiroshima University with the same method described in Yabuta et al. (2023). During drying after acid treatment, colloid-like floating materials were found, which were brownish under the microscope and sticky when handled, and are called “outlier phases” in the text. It should be noted that the IOM extraction procedures do not significantly alter the IOM, but slight modifications might occur for acid labile structures such as amides and esters (e.g., Cody et al., 2002; Kebukawa et al., 2019).

The acid residues were then transported to Yokohama National University in clean concavity glass slides. These acid residues were transferred to chemical vapor deposition diamond windows, typically 3.5 mm diameter and 0.3 mm thick, using a stainless steel needle under a binocular microscope, then pressed between two diamond windows by hand to flatten the grain surface at an appropriate thickness to avoid vibrational band saturation as well as to limit scattering effects in the transmission of irregular grains during the measurements. After separation of the two diamond windows, usually the samples are evenly distributed on both windows. The sample preparation processes are conducted under a clean hood, or a clean bench installed in a clean booth, under clean air filtered by HEPA filters.

Fourier transform infrared micro-spectroscopy (micro-FT-IR) measurements were conducted at Yokohama National University as explained in the methods described in Yabuta et al. (2023). IR absorption spectra were collected from each diamond window with a micro-FT-IR (JASCO FT/IR-6100 + IRT-5200), equipped with a ceramic IR light source, a germanium-coated KBr beam splitter, a liquid-nitrogen cooled mercury-cadmium-

telluride (MCT) detector, and $\times 16$ Cassegrain mirrors. The microscope and the FT-IR were continuously purged with dry N_2 . At each spot, 128 scans of IR transmission spectra were accumulated with a wave number resolution of 4 cm^{-1} and with a $20\text{ }\mu\text{m} \times 20\text{ }\mu\text{m}$ aperture. Optical microscope images with FT-IR analyzed spots are shown in Figure 1 and Figure S1.

Spectra from these locations are averages of 7–40 spot measurements; they are baseline-corrected using spline curves (Figure S2a) and normalized to the highest peak intensity in each spectrum. For quantitative comparisons, the peak intensities (heights), $I(\text{CH}_3)$, $I(\text{CH}_2)$, $I(\text{C}=\text{O})$, and $I(\text{C}=\text{C})$, were obtained at peak tops between 2970 and 2950 cm^{-1} for CH_3 and 2935 and 2915 cm^{-1} for CH_2 after subtracting a linear baseline between 3030 and 2770 cm^{-1} , and at peak tops between 1740 and 1700 cm^{-1} for $\text{C}=\text{O}$, and around 1620–1560 cm^{-1} for $\text{C}=\text{C}$ after subtracting a linear base between 1780 and 1485 cm^{-1} (Figure S2b–d). These calculations were performed with custom software (in Python) after smoothing (simple moving average of nine points) of each spectrum.

RESULTS

FT-IR Spectra of Acid Residues from Ryugu Particles

Figure 2 shows the average IR absorption spectra from the acid residues from Ryugu samples A0106, C0107, and C0002. Individual spectra composing these averages are presented in Figure S3. Overall, the IR spectra show variable contributions from two organic phases—one that is similar to typical IOM from unheated type 1 and 2 CCs and the other that is an outlier phase specific to each sample. The spectral characteristics of the outlier phases from A0106 and C0107 are similar, but the C0002 outlier phase shows different characteristic IR features (details given below). Mixing between chondritic-like material and the outlier phases was observed in every analysis region, and no “pure phase” spectra were found. Differences in IOM between chamber A and chamber C are not evident in the IR spectra.

Typical IOM-Like Phase

Ryugu IOM with IR spectra dominated by typical chondritic organic matter appear black under the optical microscope (Figure 1 and Figure S1). The IR absorption spectra of this typical IOM-like phase show peaks at $\sim 3400\text{ cm}^{-1}$ (OH stretching), 2960 cm^{-1} (CH_3 asymmetric stretching), $2930\text{--}2925\text{ cm}^{-1}$ (CH_2 asymmetric stretching), $2855\text{--}2850\text{ cm}^{-1}$ (CH_3 and CH_2 symmetric stretching), $\sim 1700\text{ cm}^{-1}$ (carbonyl $\text{C}=\text{O}$ stretching), $\sim 1600\text{ cm}^{-1}$ (aromatic $\text{C}=\text{C}$ stretching), and 1460 cm^{-1} (aliphatic CH bending) (Figure 2a,b). These are typical of

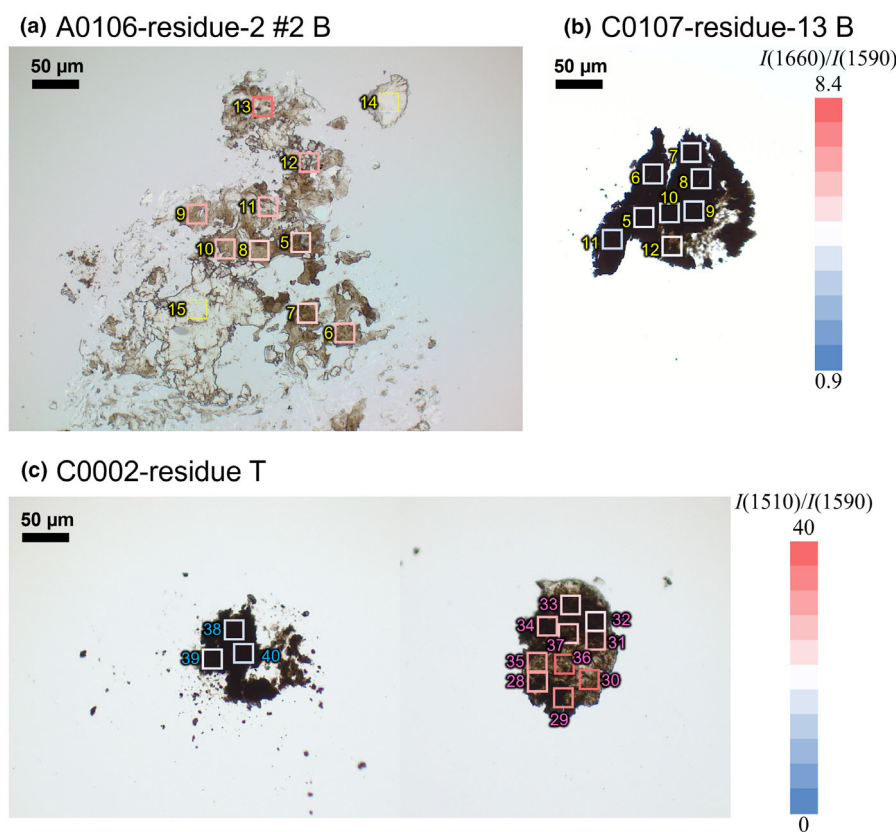


FIGURE 1. Optical microscopic images and analyzed areas indicated by squares for selected samples (a) A0106-residue-2, (b) C0107-residue-13, and (c) C0002-residue T. All images are presented in Figure S1. Analysis squares are color coded by the intensity ratios of $I(1660)/I(1590)$ for A0106 and C0107, and $I(1510)/I(1590)$ for C0002 (see the Results section for additional details). Note that the transparent materials in the A0106-residue-2 (a, spots #14 and #15) do not show IR absorption in the range of $4000\text{--}700\text{ cm}^{-1}$. These materials are likely elemental sulfur indigenous to Ryugu samples (Komatsu et al., [under review](#)). (Color figure can be viewed at [wileyonlinelibrary.com](#))

IOM from unheated type 1 and 2 CCs (Kebukawa et al., 2011; Orthous-Daunay et al., 2013; Quirico et al., 2014, 2018). In addition, a peak at 1660 cm^{-1} is observed in all spectra, which may be assigned to unsaturated ketones/aldehydes or amides. The peak at 1660 cm^{-1} is not seen in the IOM from unheated CCs but sometimes seen in the IOM from metamorphosed chondrites such as Chainpur (LL3.4) and Kainsaz (CO3.2) (Kebukawa et al., 2011). However, these metamorphosed chondrite IOM spectra do not have intense aliphatic peaks as in Ryugu IOM, and Ryugu did not experience long-term heating (Bonal et al., [under review](#); Nakamura et al., 2023; Yokoyama et al., 2023), and thus, we associate these peaks with the outlier phase. In addition, the weak absorptions at 3350 and 3180 cm^{-1} overlapped on the broad O-H band at $\sim 3300\text{ cm}^{-1}$ in the IR spectra of residues from A0106 and C0107 are not found in chondritic IOM and are similarly assigned to likely N-H stretching contributions from the outlier phase in these residues.

Peak Intensity Ratios of Typical IOM-like Phase

IR absorption spectra allow quantitative analysis of each functional group, since they follow the Lambert–

Beer law—the integrated optical depth peak intensity is proportional to the molar density, the sample thickness, and the absorption coefficient that is intrinsic to each functional group. Here, we attempt to do a first-order analysis using peak height ratios with CH_2 , CH_3 , C=O , and C=C . Because the uncertainty of sample thickness and complexity of obtaining the integrated peak intensity due to overlapping of the peaks, particularly the 1660 cm^{-1} peak which does not appear in typical IOM from CCs, makes it difficult to compare IOM from Ryugu and from CCs. Thus, we simply took peak heights at peak maxima of CH_3 at $\sim 2960\text{ cm}^{-1}$, CH_2 at $\sim 2930\text{ cm}^{-1}$, C=O at $\sim 1700\text{ cm}^{-1}$, and C=C at $\sim 1600\text{ cm}^{-1}$ after subtracting linear baselines ($3030\text{--}2770\text{ cm}^{-1}$ for CH_3 and CH_2 , and $1800\text{--}1480\text{ cm}^{-1}$ for C=O and C=C). Although a band integration is desirable, this simple approach still shows the relative abundance of each functional group and for a quick comparison between IR spectra from various laboratories. Dartois et al. (2023) showed that $I(\text{CH}_2)/I(\text{CH}_3)$ peak intensity ratios were reasonably correlated with the column density $n(\text{CH}_2)/n(\text{CH}_3)$ ratios.

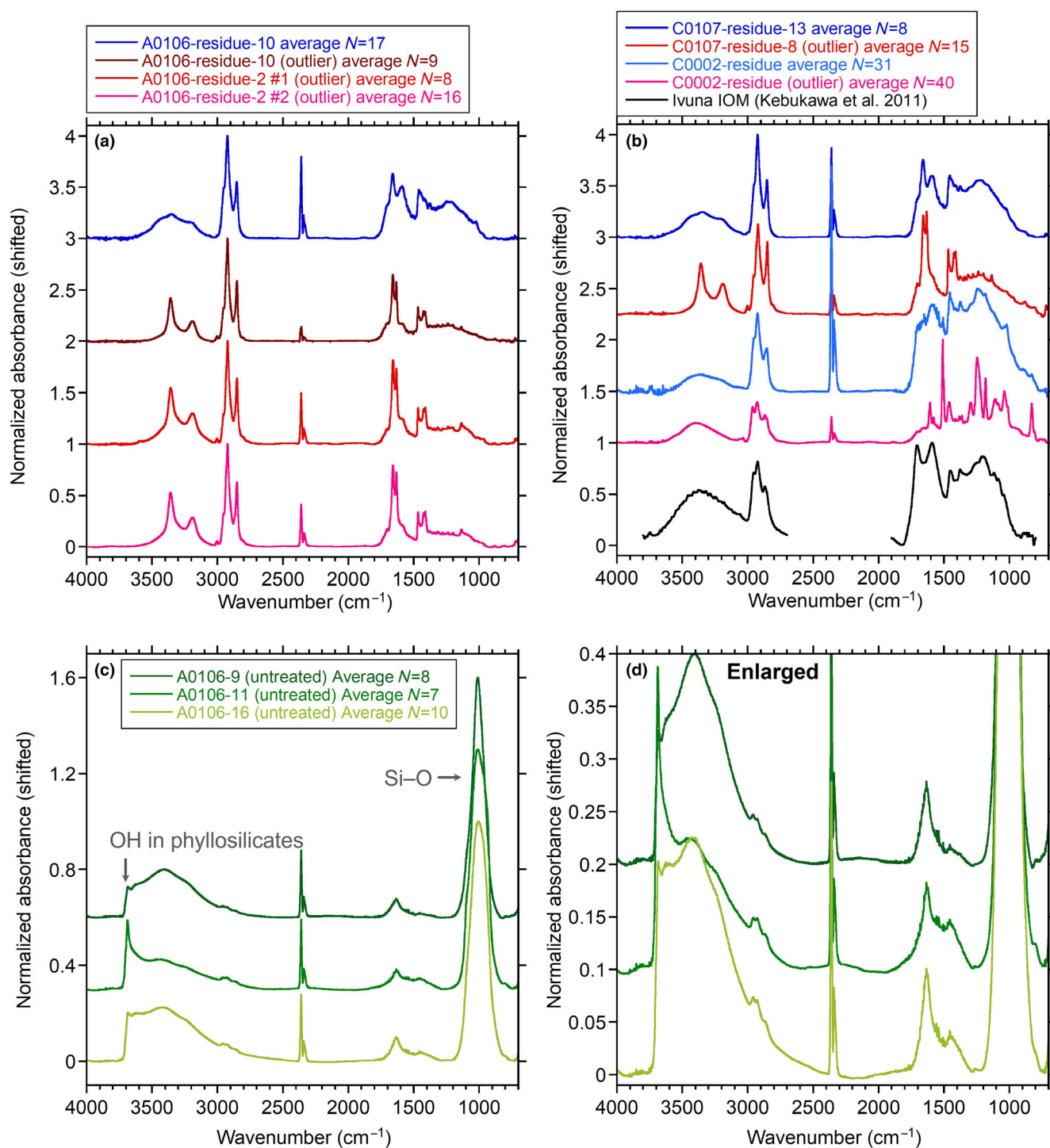
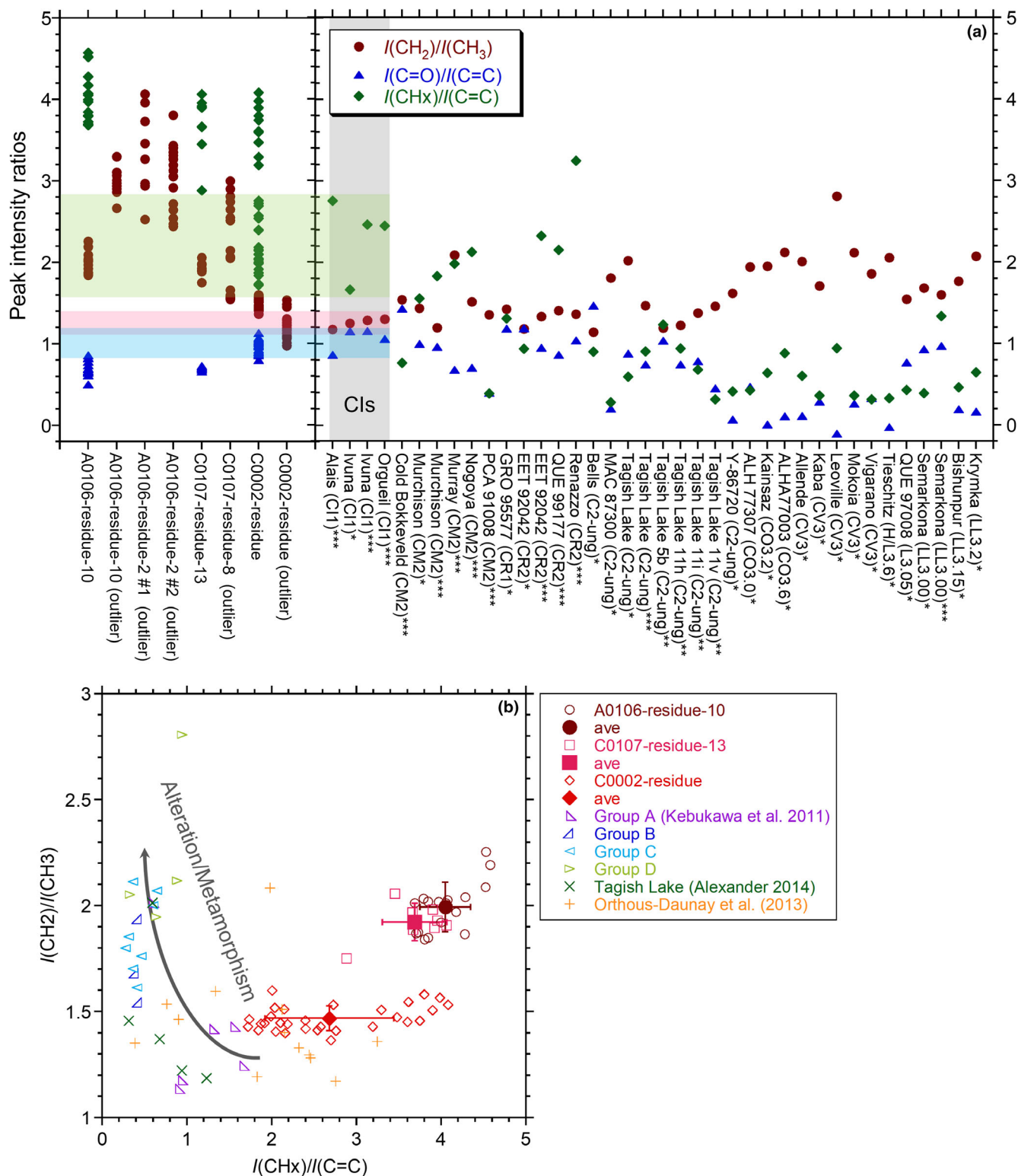


FIGURE 2. IR absorption spectra of acid residues from Ryugu samples (a) A0106, (b) C0107, and C0002 with Ivuna IOM (Kebukawa et al., 2011) for comparison, and (c) untreated particles of A0106 (with an intense phyllosilicates contribution) for comparison. Each spectrum is averaged of 7–40 analyzed spots, baseline collected, normalized by the highest peaks, and shifted for clarity. Peak assignments are shown in Table 1. The peaks at 2360 cm^{-1} are due to atmospheric CO_2 . (Color figure can be viewed at wileyonlinelibrary.com)

Figure 3a shows $I(\text{CH}_2)/I(\text{CH}_3)$, $I(\text{CH}_x)/I(\text{C}=\text{C})$, and $I(\text{C}=\text{O})/I(\text{C}=\text{C})$ peak height ratios of Ryugu acid residues compared with various chondritic IOM (Alexander

et al., 2014; Kebukawa et al., 2011; Orthous-Daunay et al., 2013). These ratios are summarized in Table S1. Note that the literature values of chondrite IOM were



recalculated based on the above methods for comparison to Ryugu IOM. The trends of the plots are not significantly affected by the methods compared to the

original plots in Kebukawa et al. (2011) and Alexander et al. (2014). It should be noted, however, that there are some differences in IOM extraction methods—our Ryugu

FIGURE 3. (a) $I(\text{CH}_2)/I(\text{CH}_3)$, $I(\text{CH}_x)/I(\text{C}=\text{C})$, and $I(\text{C}=\text{O})/I(\text{C}=\text{C})$ peak height ratios, where $I(\text{CH}_x) = I(\text{CH}_2) + I(\text{CH}_3)$, of Ryugu acid residues compared with various chondritic IOM. Green, red, and blue bands indicate the ranges of $I(\text{CH}_x)/I(\text{C}=\text{C})$, $I(\text{CH}_2)/I(\text{CH}_3)$, and $I(\text{C}=\text{O})/I(\text{C}=\text{C})$, respectively, of CI chondrites. Data from: *Kebukawa et al. (2011), **Alexander et al. (2014), ***Orthous-Daunay et al. (2013). (b) $I(\text{CH}_x)/I(\text{C}=\text{C})$ ratios versus $I(\text{CH}_2)/I(\text{CH}_3)$ ratios. Groups A–D are IR spectral groups of chondrite IOM as defined by Kebukawa et al. (2011): Group A includes unheated type 1 and 2 CCs, Group B has slightly heated chondrites, and Groups C and D include moderately heated chondrites. The arrow indicates the alteration/metamorphism trend. (Color figure can be viewed at wileyonlinelibrary.com)

samples and those of Orthous-Daunay et al. (2013) were prepared with HF/HCl whereas Kebukawa et al. (2011) and Alexander et al. (2014) used CsF/HF. This difference may affect the molecular structures of IOM residues, for example, $\text{CH}_x/\text{C}=\text{C}$ ratios in the IOM obtained from HF/HCl tend to be higher than these from CsF/HF (see Ivuna, Murchison, EET 92042, and Semarkona in Figure 3a). However, the $I(\text{CH}_2)/I(\text{CH}_3)$ peak height ratios of typical IOM-like phase are consistent with the peak height ratios of intact Ryugu particles reported by Dartois et al. (2023).

Since Ryugu is most similar petrologically to CI chondrites (Nakamura et al., 2023; Yokoyama et al., 2023), it is particularly interesting to find marked differences in IR peak intensities between Ryugu IOM and CI IOM. The IOM from Ryugu samples A0106 and C0107 (except outlier residues) has higher $I(\text{CH}_2)/I(\text{CH}_3)$ and $I(\text{CH}_x)/I(\text{C}=\text{C})$ ratios and lower $I(\text{C}=\text{O})/I(\text{C}=\text{C})$ ratios compared to CI IOM. The IOM from C0002 is relatively closer to CI IOM compared to A0106 and C0107. Figure 3b shows $I(\text{CH}_2)/I(\text{CH}_3)$ ratios versus $I(\text{CH}_x)/I(\text{C}=\text{C})$ ratios of the typical IOM-like phase from Ryugu samples compared with IOM from various chondrites (Alexander et al., 2014; Kebukawa et al., 2011; Orthous-Daunay et al., 2013). In the case of IOM from chondrites, the $I(\text{CH}_x)/I(\text{C}=\text{C})$ ratios decrease, and the $I(\text{CH}_2)/I(\text{CH}_3)$ increases with increasing parent body alteration/metamorphism. Ryugu IOM plots outside of these trends—both the measured $I(\text{CH}_x)/I(\text{C}=\text{C})$ and $I(\text{CH}_2)/I(\text{CH}_3)$ ratios were higher than those of unheated type 1 and 2 CCs.

Outlier Phases

Outlier Phase from A0106 and C0107

Analysis regions containing a higher proportion of the outlier organic phase in samples A0106 and C0107 appear transparent light brown (Figure 1 and Figure S1). The IR absorption spectra from outlier phases from A0106 and C0107 are significantly different from the typical IOM-like phases (Figure 2 and Figure S3). They contain characteristic peaks at 3350 and 3180 cm^{-1} assigned to N-H stretching modes, along with sharp peaks at 1660 and 1630 cm^{-1} , and weaker peaks at 1465, 1420, and 1410 cm^{-1} . Aliphatic C-H stretching features

at $\sim 2900 \text{ cm}^{-1}$ are similar to typical IOM-like material, but an aromatic C-H peak at 3005 cm^{-1} is obvious in these outlier phases although it is small. A database search using the Spectral Database for Organic Compounds (SDBS; https://sdb.sdb.aist.go.jp/sdb/cgi-bin/direct_frame_top.cgi) provided by the National Institute of Advanced Industrial Science and Technology (AIST), Japan, for these additional peak positions returned matches to aliphatic primary amines, for example, octanamide ($\text{C}_8\text{H}_{17}\text{NO}$), myristamide ($\text{C}_{14}\text{H}_{29}\text{NO}$), oleamide ($\text{C}_{18}\text{H}_{35}\text{NO}$), and cis-11-icosenamide ($\text{C}_{20}\text{H}_{39}\text{NO}$). This result does not mean that the outlier phase from A0106 and C0107 is comprised of one of these specific compounds, but rather indicates that the phase shares similar chemical structures with these compounds. Aside from amino functional groups, the outlier phase in A0106 and C0107 should also contain aromatic moieties, as observed in the IR spectra.

Estimation of $n(\text{NH}_2)/n(\text{CH}_x)$ Molar Ratios

We estimated $n(\text{NH}_2)/n(\text{CH}_x)$ molar ratios using as a reference spectrum an aliphatic primary amide—hexanamide. The $A(\text{NH})/A(\text{CH}_x)$ peak area ratios of outlier phases from A0106 and C0107 were calculated using the band contributions from N-H stretching modes in the 3560–3030 cm^{-1} range and in the 2990–2770 cm^{-1} range for the C-H stretching modes (Figure 4). The band ratios of $A(\text{NH})/A(\text{CH}_x)$ were then converted to $n(\text{NH}_2)/n(\text{CH}_x)$ molar ratios using the $A(\text{NH})/A(\text{CH}_x)$ peak area ratio of hexanamide considering it possesses one NH_2 for five CH_x (four CH_2 and one CH_3):

$$n(\text{NH}_2)/n(\text{CH}_x) = (1/5) \cdot [A(\text{NH})/A(\text{CH}_x)] / [A(\text{NH})/A(\text{CH}_x)]_{\text{hexanamide}}$$

The results are shown in Table S1. Assuming that the outlier phases are aliphatic primary amide-like compounds, they contain about 14–24 aliphatic carbon per NH_2 . Also, in a similar manner to using $I(\text{CH}_2)/I(\text{CH}_3)$ ratios, the $n(\text{CH}_2)/n(\text{CH}_3)$ molar ratios can be estimated to be approximately 9–13, indicating that the outlier phases contain one or two CH_3 per one NH_2 . The lack of short-chain amides could be due to loss of short-chain amides during solvent extraction process by the SOM IAT conducted prior to our acid treatment.

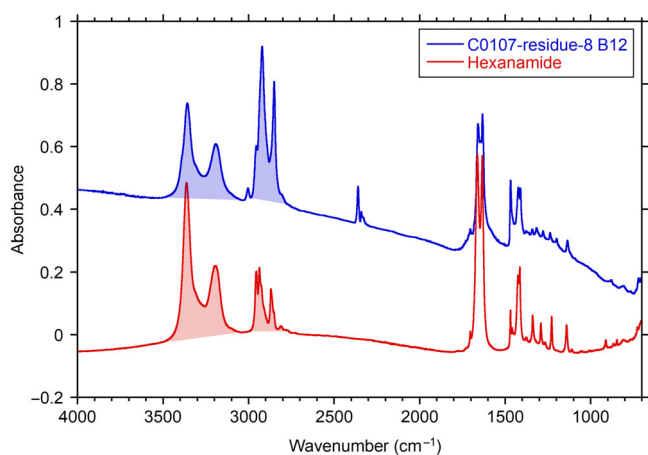


FIGURE 4. IR absorption spectra of hexanamide reference (red) and C0107-residue-8 (blue). Shadow areas indicate $A(\text{NH})$ (3560–3030 cm^{-1}) and $A(\text{CH}_x)$ (2990–2770 cm^{-1}). (Color figure can be viewed at [wileyonlinelibrary.com](https://onlinelibrary.wiley.com/doi/10.1111/maps.14064))

Soluble amide compounds have not been detected from Ryugu samples so far (Naraoka et al., 2023). This calculation focuses on a small set of IR peaks in the entire spectrum, and the macromolecular residues contain other functional groups and have more complex molecular structures. In particular, a small aromatics contribution is present in the outlier phases as discussed above with an aromatic C-H peak at $\sim 3005 \text{ cm}^{-1}$.

Outlier Phase from C0002

Analysis regions with a higher proportion of the outlier phase in sample C0002 appear dark brown (Figure 1 and Figure S1). The IR absorption spectra from the outlier phase in C0002 are significantly different from both the typical IOM-like material and outlier phase from A0106 and C0107 (Figure 2 and Figure S3). The outlier phase from C0002 has characteristic peaks at 1510, 1245, 1180, and 830 cm^{-1} , with smaller peaks at 1605, 1460, 1295, 1110, and 1040 cm^{-1} (Table 1). Aliphatic C-H stretching features at $\sim 2900 \text{ cm}^{-1}$ are contributed by typical IOM-like phases but with lower CH_2/CH_3 ratios. The peaks at 1605–1510 cm^{-1} are in the range of aromatic C=C stretching, 1460 cm^{-1} is in the range of aliphatic C-H bending, 1295–1040 cm^{-1} are in the range of C-O stretching, and 830 cm^{-1} is in the range of aromatic/olefinic C-H bending. Unlike the outlier phase from A0106 and C0107, a SDBS search did not provide match results, but the best match compound is 4'-methoxyacetophenone (Scheme 1). This database match indicates that the outlier phase in C0002 likely contains a combination of phenyl, methyl, methylene, ether, and ketone groups.

This distribution of functional groups is similar to that of the “Aromatic” organic grains observed in both

Ryugu untreated particles and IOM in carbon X-ray absorption near-edge structure (C-XANES) spectra (Yabuta et al., 2023). The XANES spectra of these grains contain an uncharacteristically narrow aromatic peak at 285 eV relative to other organic matter in the Ryugu samples, along with a broad absorption between 288 and 289 eV consistent with abundant aliphatic bonding. Such C-XANES features are not seen in CCs and indicate small aromatic domains substituted and bridged with carboxyl and aliphatic functional groups (Yabuta et al., 2023).

Distributions of Outlier Phases

The characteristic peaks of both chondritic IOM-like phases and the outlier phases can be used to estimate their relative abundances in each analysis region. Thus, we took peak height ratios of $I(1660 \text{ cm}^{-1})/I(1590 \text{ cm}^{-1})$ for samples A0106 and C0107 and $I(1510 \text{ cm}^{-1})/I(1590 \text{ cm}^{-1})$ for sample C0002, where 1590 cm^{-1} is the C=C peak position in IOM-like phases. The color scales shown in Figure 1 and Figure S1 indicate the peak height ratios of $I(1660 \text{ cm}^{-1})/I(1590 \text{ cm}^{-1})$ in A0106 and C0107 samples and $I(1510 \text{ cm}^{-1})/I(1590 \text{ cm}^{-1})$ in C0002 samples. The peak height ratios are listed in Table S1. Overall, outlier phases show brighter colors in optical images, although appearance under the optical microscope also depends on sample thickness. However, transparent phases do not show IR absorption bands in the range of 4000–700 cm^{-1} (Figure 1 and Figure S3).

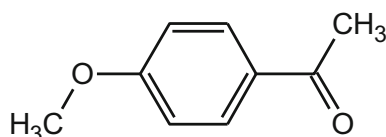
Comparison of FT-IR Spectra of Acid Residues and Untreated Ryugu Particles

IR absorption spectra from untreated particles from A0106 (Figure 2c) show similar spectral features to the IR spectra from typical Ryugu untreated particles which are consistent with CI chondrites (Dartois et al., 2023; Yabuta et al., 2023). Because of the relatively small amount of outlier phases compared to typical IOM-like phases, it is reasonable that they are not seen in the IR spectra of the untreated sample. Although there are no N-H peaks in our untreated Ryugu analyzed samples, N-H absorption bands were previously reported from reflectance IR measurements of a few N-rich untreated Ryugu particles by two individual instruments at JAXA Curation (Pilorget et al., 2022; Yada et al., 2022). Based on X-ray diffraction, Viennet et al. (2023) suggested that organics trapped within the interlayer space of smectite might explain the N-H peaks in the IR spectra of Ryugu samples. Yada et al. (2022) showed peaks at 3.1 μm (3226 cm^{-1}), while Pilorget et al. (2022) showed a peak at 3.06 μm (3268 cm^{-1}) with a weaker peak at 3.24 μm (3086 cm^{-1}). The differences in peak positions between Ryugu residues observed in this study and untreated particles observed by the curation team might be

TABLE 1. Assignments of the IR features in the Ryugu acid residues.

Wave number (cm ⁻¹)	Implied functional group	Typical IOM-like phases		Outlier phases		Untreated A0106
		A0106&C0107	C0002	A0106&C0107	C0002	
3685	OH inorganic					++
~3400–3300	O–H stretching, organic/water	+	+		+	++
3350	N–H stretching	+		++		
3180	N–H stretching	+		++		
3005	C–H stretching, aromatic/olefinic			+	+	
2960	CH ₃ asymmetric stretching	+	+	+	++	+
2930–2925	CH ₂ asymmetric stretching	++	++	++	++	+
2855–2850	CH ₃ and CH ₂ symmetric stretching	++	++	++	++	+
~1700	C=O stretching	++	+	+	+	
1660	C=O stretching	++	+	++	+	
1635	Aromatic C=C stretching			++		++
1605	Aromatic C=C stretching				++	
~1590	Aromatic C=C stretching	++	++	++	+	+
1510	Aromatic C=C stretching		++		++	
1460	Aliphatic C–H bending	++	++	++	++	
~1450	Carbonates					++
1420–1410	Aliphatic C–H bending	+		++	+	
1375	Aliphatic C–H bending	+	++	+	+	
1295	C–O stretching				++	
1245	C–O stretching		++		++	
1180	C–O stretching		+		++	
1110	C–O stretching				++	
~1000	Si–O stretching					++
1040–1020	C–O stretching	+	++	+	++	
830	C–H bending, aromatic/olefinic		+		++	

Note: ++, strong; +, minor.



SCHEME 1. 4'-methoxyacetophenone (4-acetylanisole).

attributed to alteration of N-H-bearing phases during the acid treatment, since the N-H containing functional groups are likely susceptible to acids, although we cannot fully exclude the possibility of alteration by solvents during SOM extraction.

DISCUSSION

Possible Sources of Outlier Phases

Here, we consider various sources of potential organic contaminations to explain the presence of outlier phases in the Ryugu IOM residues. The antigorite blank prepared by acid treatments at the same time with A0106 and C0107 contains no residual organic matter. In

addition, outlier IR spectra have not been observed in CCs, but are ubiquitously found in Ryugu samples A0106, C0107, and C0002. It is also worth noting that presolar SiC grains were found embedded in the outlier phase (Barosch et al., 2022), supporting that the indigenous nature of the outlier phase. Thus, we can exclude the possibility of contamination during acid IOM extraction treatment and IR measurement procedures.

The sampling from Ryugu used projectiles with explosives to collect the samples into the sampler horn (Sawada et al., 2017). FT-IR spectra from possible projectiles and explosives contaminants (Ito et al., 2021; Takano et al., 2020) do not match with the outlier phases (Figure 5). Some likely artificial organic particles were found in the Hayabusa sample container (Uesugi et al., 2014; Yada et al., 2014). The IR spectra of these particles (Kitajima et al., 2015) also do not match with the outlier phases reported here. Thus, these outlier phases in our Ryugu samples were not introduced during sampling at Ryugu by the Hayabusa2 spacecraft.

In the case of the outlier phases from A0106 and C0107, aliphatic amide compounds may imply compounds used in cell membranes, such as ceramides. Human skin

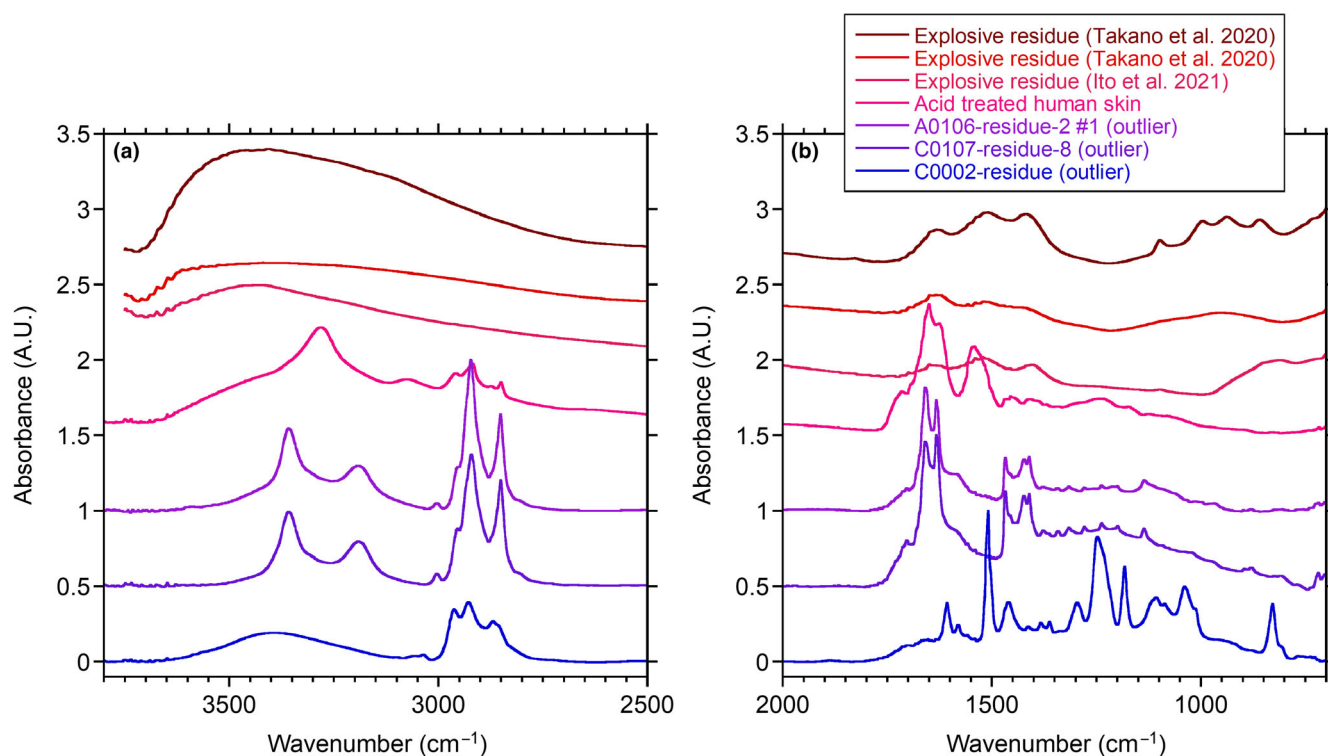


FIGURE 5. IR absorption spectra of possible contaminations compared to the outlier phases from Ryugu acid residues for (a) 3800–2500 cm^{-1} and (b) 2000–700 cm^{-1} regions. (Color figure can be viewed at wileyonlinelibrary.com)

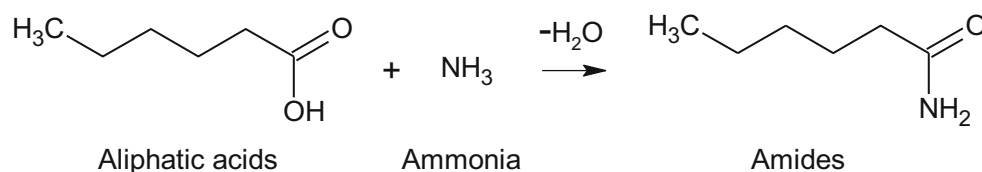
could be a possible contamination source during sample handling procedures. Considering that amide bonds are hydrolyzed by acids, a human skin sample was treated with HF/HCl, then subjected to FT-IR analysis. The IR absorption spectrum of HF/HCl-treated human skin is compared to Ryugu outlier acid residues (Figure 5). The characteristic peaks at 1540 and 3280 cm^{-1} in the human skin are missing in the spectra of the outlier phases from A0106 and C0107, although a bimodal peak at $\sim 1650 \text{ cm}^{-1}$ is common in both the human skin and the outlier phases.

In the case of the outlier phase in C0002, the best match compound from the database is 4'-methoxyacetophenone (4-acetylanisole), which is used as a perfume and flavoring ingredient. Our clean sample processing protocols eliminate the likelihood that a perfume/flavoring ingredient contaminated our Ryugu samples pervasively at a detectable level.

Differences Between Ryugu and Unheated Type 1 and 2 CCs

Ryugu IOM falls outside of the aliphatic peak intensity trends for unheated type 1 and 2 CCs, as both $I(\text{CH}_2)/I(\text{CH}_3)$ ratios and $I(\text{CH}_x)/I(\text{C}=\text{C})$ ratios measured are higher, particularly in the case of A0106 and C0107

(Figure 3). The C0002 IOM falls closer to the unheated type 1 and 2 CCs, particularly similar to the IOM from Orthous-Daunay et al. (2013) which was prepared by the HF/HCl method used here, but has slightly higher $I(\text{CH}_x)/I(\text{C}=\text{C})$ ratios. In contrast, $\text{C}=\text{O}/\text{C}=\text{C}$ ratios of Ryugu IOM are similar to unheated chondrites. Increases in the CH_2/CH_3 ratios are usually attributed to thermal processing (Kebukawa et al., 2011; Orthous-Daunay et al., 2013; Quirico et al., 2018), but Raman spectra of Ryugu untreated particles exclude the possibility of heating, with the possible exception of a few rare particles (Bonal et al., [under review](#); Komatsu et al., [under review](#)), and the higher $\text{CH}_x/\text{C}=\text{C}$ ratios also suggest an unheated nature. High CH_2/CH_3 ratios have also been reported in primitive IDPs and considered as reflecting less altered nature of such IDPs compared to chondrites (Flynn et al., 2003, 2008). The high $I(\text{CH}_2)/I(\text{CH}_3)$ ratios of A0106 and C0107 could be due to some contributions of the outlier phases, since these phases from A0106 and C0107 have obviously high $I(\text{CH}_2)/I(\text{CH}_3)$ ratios (Figure 2a), although the plot of $I(\text{CH}_2)/I(\text{CH}_3)$ versus $I(\text{CH}_x)/I(\text{C}=\text{C})$ ratios in Figure 3b excluded the outlier phases. The high $I(\text{CH}_x)/I(\text{C}=\text{C})$ ratios of Ryugu IOM may imply (1) intrinsic differences in nature, origin/evolutional history of Ryugu IOM, and/or (2) less



SCHEME 2. Amides production from carboxylic acids and ammonia or amines.

terrestrial residential time and thus a higher degree of preservation when compared to the previously measured unheated CCs. Yokoyama et al. (2023) suggested that the organic matter in CI chondrites would be affected by oxidation. Oxidative degradation of organic matter in CCs may lead to loss of hydrogen as seen in terrestrial sedimental organic matter (e.g., Ganz & Kalkreuth, 1991; Hutton et al., 1994). Thus, IOM from unheated CCs might originally have higher $\text{CH}_x/\text{C}=\text{C}$ ratios. Orgueil fell in 1864 and Ivuna in 1938, so long-term exposures to terrestrial environments may slowly decrease aliphatic moieties. Meanwhile, Quirico et al. (under review) reported FT-IR data for different IOM residues from Ryugu and found that they were generally consistent with CI chondrites, with some heterogeneities, and did not find outlier phases. Such differences could be attributed to the small sample amount used in Quirico et al., and the differences in SOM and IOM extraction procedures—A0106 and C0107 were subjected to comprehensive SOM extraction, but sample heterogeneities cannot be ruled out.

An important point to consider in comparing Ryugu samples to CCs is the potential difference between the sampling depth from the parent bodies. Ryugu particles were sampled at the surface; ~50% were taken from <1.5 mm from the surface (also possibly including some subsurface materials from ~1 m in depth for the chamber C sample; Tachibana et al., 2022). However, material within tens of centimeter of a meteoroid's surface would have been lost during atmospheric entry (Velbel & Zolensky, 2021); thus, CCs are expected to come from deeper, at least several centimeters, in their parent bodies. Thus, the organic matter in Ryugu samples might have experienced different chemical processing histories compared to the organic matter recorded in CCs fallen on Earth. Surface processes include the effects of UV photons and energetic particles (galactic and solar cosmic rays). UV and solar wind penetrate only a few tens to hundred nanometers, whereas solar energetic particles (H^+) can penetrate to >100 μm , and even up to tens of centimeter for the less abundant galactic cosmic rays depending on their energy (Bennett et al., 2013). Micrometeorite impacts may have also delivered locally large energy input at the surface of Ryugu. Some Ryugu

particles have surfaces with molten features and/or with melt splashes, most likely formed by micrometeoroid bombardment (Noguchi et al., 2023). Long-term irradiation of porous surface materials may induce enough alteration of organics of the Ryugu samples. However, UV and energetic particles likely induce loss of hydrogen and increase (or does not change) $\text{C}=\text{C}$ bonds (Muñoz Caro et al., 2006; Ogmen & Duley, 1988; Orthous-Daunay et al., 2019). Thus, the effects of such irradiations do not explain the high aliphatic/aromatic ratios in Ryugu samples, unless such energetic processes would mobilize highly aliphatic SOM to convert it to macromolecular IOM.

Formation of Amides at the Surface of Asteroids

Amide compounds can be synthesized by dehydration of carboxylic acids with ammonia or amines (Scheme 2). At the near surfaces of asteroids, sublimation of ice containing carboxylic acids and amines (or amine salts) could produce residues of amides. Or, if amines are not very abundant, fluids containing carboxylic acids and ammonia could produce ammonium carboxylates at the interior of asteroids. At the near surface of asteroids, ammonia and amines may exist in phyllosilicates and/or as salts, as observed in dwarf planet 1 Ceres (De Sanctis et al., 2015) and comet 26P/Grigg-Skjellerup (Altwegg et al., 2020). Furthermore, Poch et al. (2020) showed that ammonium salts, such as ammonium formate, matched well with the spectra of the surface of nucleus of comet 67P/Churyumov-Gerasimenko, as well as some asteroids. It is plausible that ammonia was abundant in Ryugu since CO_2 -bearing fluid inclusions in Ryugu suggest that Ryugu's parent asteroid originally formed in the outer solar system before moving to the current orbit (Nakamura et al., 2023). Evidence of N-bearing organic compounds was also found in these fluid inclusions (Nakamura et al., 2023). As the fluid moved from the interior to the subsurface of the asteroid, water would have been lost through evaporation, but amide compounds may have remained. Aliphatic amines (likely in the form of salts) and carboxylic acids were detected in the Ryugu A0106 sample, but the abundances were smaller than those reported in the Murchison meteorite (Naraoka et al., 2023). The depletion of amines and carboxylic acids in Ryugu

might be explained by the consumption of these molecules by the formation of amides. It is worth noting that amide compounds were abundantly produced from laboratory irradiation experiments on icy dust particles simulating interstellar or cometary dust (e.g., Briggs et al., 1992).

CONCLUSIONS

The FT-IR absorption spectra of acid residues from Ryugu samples show mainly three different phases: (1) similar to typical IOM from unheated CCs, (2) outlier phases with characteristic N-bearing bands, and (3) outlier phases with no clear N-related features. The typical IOM-like phases do not show signatures of heating (either short- or long-term heating) and have higher aliphatic/aromatic ratios and CH₂/CH₃ ratios compared to IOM from unheated CCs. Such characteristics could be due to the freshness of the Ryugu sample compared to CCs with longer terrestrial residential periods, but one cannot exclude the possibility of contributions from outlier phases with high CH₂/CH₃ ratios. The N-bearing outlier phases were found in both A0106 and C0107, and likely contain amide functional groups. These phases might be the results of near-surface processes of Ryugu, but more studies are required to elucidate their origin. The other outlier phases were only found in C0002, and contain phenyl, methyl, methylene, ether, and ketone functional groups, but the detailed nature is not well identified.

Acknowledgments—Shin-ichiro Mochizuki is acknowledged for providing IR data processing program in Python. Y.K. was supported by Japan Society for the Promotion of Science KAKENHI (grant numbers JP17H06458; JP19H05073; JP21H00036).

Data Availability Statement—The data that support the findings of this study are available from the corresponding author upon reasonable request.

Editorial Handling—Dr. Daniel Patrick Glavin

REFERENCES

Alexander, C. M. O'D., Cody, G. D., Kebukawa, Y., Bowden, R., Fogel, M. L., Kilcoyne, A. L. D., Nittler, L. R., and Herd, C. D. K. 2014. Elemental, Isotopic, and Structural Changes in Tagish Lake Insoluble Organic Matter Produced by Parent Body Processes. *Meteoritics & Planetary Science* 49: 503–525.

Altwegg, K., Balsiger, H., Hänni, N., Rubin, M., Schuhmann, M., Schroeder, I., Sémon, T., et al. 2020. Evidence of Ammonium Salts in Comet 67P as Explanation for the Nitrogen Depletion in Cometary Comae. *Nature Astronomy* 4: 533–540.

Arakawa, M., Saiki, T., Wada, K., Ogawa, K., Kadono, T., Shirai, K., Sawada, H., et al. 2020. An Artificial Impact

on the Asteroid (162173) Ryugu Formed a Crater in the Gravity-Dominated Regime. *Science* 368: 67–71.

Barosch, J., Nittler, L. R., Wang, J., Alexander, C. M. O'D., De Gregorio, B. T., Engrand, C., Kebukawa, Y., et al. 2022. Presolar Stardust in Asteroid Ryugu. *The Astrophysical Journal Letters* 935: L3.

Battandier, M., Bonal, L., Quirico, E., Beck, P., Engrand, C., Duprat, J., and Dartois, E. 2018. Characterization of the Organic Matter and Hydration State of Antarctic Micrometeorites: A Reservoir Distinct from Carbonaceous Chondrites. *Icarus* 306: 74–93.

Beck, P., Garenne, A., Quirico, E., Bonal, L., Montes-Hernandez, G., Moynier, F., and Schmitt, B. 2014. Transmission Infrared Spectra (2–25μm) of Carbonaceous Chondrites (CI, CM, CV–CK, CR, C2 Ungrouped): Mineralogy, Water, and Asteroidal Processes. *Icarus* 229: 263–277.

Beck, P., Quirico, E., Montes-Hernandez, G., Bonal, L., Bollard, J., Orthous-Daunay, F. R., Howard, K. T., et al. 2010. Hydrous Mineralogy of CM and CI Chondrites from Infrared Spectroscopy and their Relationship with Low Albedo Asteroids. *Geochimica et Cosmochimica Acta* 74: 4881–92.

Bennett, C. J., Pirim, C., and Orlando, T. M. 2013. Space-Weathering of Solar System Bodies: A Laboratory Perspective. *Chemical Reviews* 113: 9086–9150.

Bonal, L., Alexander, C. M. O'D., Huss, G. R., Nagashima, K., Quirico, E., and Beck, P. 2013. Hydrogen Isotopic Composition of the Water in CR Chondrites. *Geochimica et Cosmochimica Acta* 106: 111–133.

Bonal, L., Quirico, E., Montagnac, G., Komatsu, M., Kebukawa, Y., Yabuta, H., Amano, K., et al. The Thermal History of Ryugu Based on Raman Characterization of Hayabusa2 Samples. *Icarus*. Under review.

Briani, G., Quirico, E., Gounelle, M., Paulhiac-Pison, M., Montagnac, G., Beck, P., Orthous-Daunay, F. R., et al. 2013. Short Duration Thermal Metamorphism in CR Chondrites. *Geochimica et Cosmochimica Acta* 122: 267–279.

Briggs, R., Ertem, G., Ferris, J. P., Greenberg, J. M., McCain, P. J., Mendoza-Gomez, C. X., and Schutte, W. 1992. Comet Halley as an Aggregate of Interstellar Dust and Further Evidence for the Photochemical Formation of Organics in the Interstellar Medium. *Origins of Life and Evolution of the Biosphere* 22: 287–307.

Brunetto, R., Borg, J., Dartois, E., Rietmeijer, F. J. M., Grossemy, F., Sandt, C., Le Sergeant d'Hendecourt, L., et al. 2011. Mid-IR, Far-IR, Raman Micro-Spectroscopy, and FESEM–EDX Study of IDP L2021C5: Clues to its Origin. *Icarus* 212: 896–910.

Chan, Q. H. S., Stroud, R., Martins, Z., and Yabuta, H. 2020. Concerns of Organic Contamination for Sample Return Space Missions. *Space Science Reviews* 216: 56.

Cody, G. D., Alexander, C. M. O. D., and Tera, F. 2002. Solid-State (H-1 and C-13) Nuclear Magnetic Resonance Spectroscopy of Insoluble Organic Residue in the Murchison Meteorite: A Self-Consistent Quantitative Analysis. *Geochimica et Cosmochimica Acta* 66: 1851–65.

Dartois, E., Engrand, C., Brunetto, R., Duprat, J., Pino, T., Quirico, E., Remusat, L., et al. 2013. UltraCarbonaceous Antarctic Micrometeorites, Probing the Solar System beyond the Nitrogen Snow-Line. *Icarus* 224: 243–252.

Dartois, E., Engrand, C., Duprat, J., Godard, M., Charon, E., Delauche, L., Sandt, C., and Borondics, F. 2018. Dome C

- Ultracarbonaceous Antarctic Micrometeorites. *Click here to enter text.* 609: A65.
- Dartois, E., Kebukawa, Y., Yabuta, H., Mathurin, J., Engrand, C., Duprat, J., Bejach, L., et al. 2023. Chemical Composition of Carbonaceous Asteroid Ryugu from Synchrotron Spectroscopy in the Mid- to Far-Infrared of Hayabusa2-Returned Samples. *A&A* 671: A2.
- De Sanctis, M. C., Ammannito, E., Raponi, A., Marchi, S., McCord, T. B., McSween, H. Y., Capaccioni, F., et al. 2015. Ammoniated Phyllosilicates with a Likely Outer Solar System Origin on (1) Ceres. *Nature* 528: 241–44.
- Flynn, G., Keller, L., Wirick, S., and Jacobsen, C. 2008. Organic Matter in Interplanetary Dust Particles. *Proceedings of the International Astronomical Union* 4: 267–276.
- Flynn, G. J., Keller, L. P., Feser, M., Wirick, S., and Jacobsen, C. 2003. The Origin of Organic Matter in the Solar System: Evidence from the Interplanetary Dust Particles. *Geochimica et Cosmochimica Acta* 67: 4791–4806.
- Ganz, H. H., and Kalkreuth, W. 1991. IR Classification of Kerogen Type, Thermal Maturation, Hydrocarbon Potential and Lithological Characteristics. *Journal of Southeast Asian Earth Sciences* 5: 19–28.
- Hutton, A., Bharati, S., and Robl, T. 1994. Chemical and Petrographic Classification of Kerogen/Macerals. *Energy & Fuels* 8: 1478–88.
- Ito, M., Takano, Y., Kebukawa, Y., Ohigashi, T., Matsuoka, M., Kiryu, K., Uesugi, M., et al. 2021. Assessing the Debris Generated by the Small Carry-on Impactor Operated from the Hayabusa2 Mission. *Geochemical Journal* 55: 223–239.
- Kebukawa, Y., Alexander, C. M. O'D., and Cody, G. D. 2011. Compositional Diversity in Insoluble Organic Matter in Type 1, 2 and 3 Chondrites as Detected by Infrared Spectroscopy. *Geochimica et Cosmochimica Acta* 75: 3530–41.
- Kebukawa, Y., Alexander, C. M. O'D., and Cody, G. D. 2019. Comparison of FT-IR Spectra of Bulk and Acid Insoluble Organic Matter in Chondritic Meteorites: An Implication for Missing Carbon during Demineralization. *Meteoritics & Planetary Science* 54: 1632–41.
- Keller, L. P., Messenger, S., Flynn, G. J., Clemett, S., Wirick, S., and Jacobsen, C. 2004. The Nature of Molecular Cloud Material in Interplanetary Dust. *Geochimica et Cosmochimica Acta* 68: 2577–89.
- Kitajima, F., Uesugi, M., Karouji, Y., Ishibashi, Y., Yada, T., Naraoka, H., Abe, M., et al. 2015. A Micro-Raman and Infrared Study of Several Hayabusa Category 3 (Organic) Particles. *Earth Planets Space* 67: 20.
- Komatsu, M., Yabuta, H., Kebukawa, Y., Bonal, L., Quirico, E., Fagan, T., Cody, G. D., et al. Examination of Laser-Induced Fluorescence from Ryugu Particles and Their Extracted Carbonaceous Residues by Raman Spectroscopy. *Meteoritics and Planetary Science*. Under review.
- Martins, Z., Hofmann, B. A., Gnos, E., Greenwood, R. C., Verchovsky, A., Franchi, I. A., Jull, A. J. T., et al. 2007. Amino Acid Composition, Petrology, Geochemistry, C-14 Terrestrial Age and Oxygen Isotopes of the Sh₂ 033 CR Chondrite. *Meteoritics & Planetary Science* 42: 1581–95.
- Matrajt, G., Caro, G. M. M., Dartois, E., d'Hendecourt, L., Deboffle, D., and Borg, J. 2005. FTIR Analysis of the Organics in IDPs: Comparison with the IR Spectra of the Diffuse Interstellar Medium. *Astronomy & Astrophysics* 433: 979–995.
- Muñoz Caro, G. M., and Dartois, E. 2009. A Tracer of Organic Matter of Prebiotic Interest in Space, Made from UV and Thermal Processing of Ice Mantles. *Astronomy & Astrophysics* 494: 109–115.
- Muñoz Caro, G. M., Matrajt, G., Dartois, E., Nuevo, M., d'Hendecourt, L., Deboffle, D., Montagnac, G., Chauvin, N., Boukari, C., and Du, D. L. 2006. Nature and Evolution of the Dominant Carbonaceous Matter in Interplanetary Dust Particles: Effects of Irradiation and Identification with a Type of Amorphous Carbon. *Astronomy and Astrophysics* 459: 147–159.
- Nakamura, T., Matsumoto, M., Amano, K., Enokido, Y., Zolensky, M. E., Mikouchi, T., Genda, H., et al. 2023. Formation and Evolution of Carbonaceous Asteroid Ryugu: Direct Evidence from Returned Samples. *Science* 379: eabn8671.
- Naraoka, H., Takano, Y., Dworkin, J. P., Oba, Y., Hamase, K., Furusho, A., Ogawa, N. O., et al. 2023. Soluble Organic Molecules in Samples of the Carbonaceous Asteroid (162173) Ryugu. *Science* 379: eabn 9033.
- Noguchi, T., Matsumoto, T., Miyake, A., Igami, Y., Haruta, M., Saito, H., Hata, S., et al. 2023. A Dehydrated Space-Weathered Skin Cloaking the Hydrated Interior of Ryugu. *Nature Astronomy* 7: 170–181.
- Ogmen, M., and Duley, W. W. 1988. Laboratory Synthesis of Hydrogenated Amorphous Carbon Films. *The Astrophysical Journal* 334: L117.
- Orthous-Daunay, F.-R., Piani, L., Flandinet, L., Thissen, R., Wolters, C., Vuitton, V., Poch, O., Moynier, F., Sugawara, I., and Naraoka, H. 2019. Ultraviolet-Photon Fingerprints on Chondritic Large Organic Molecules. *Geochemical Journal* 53: 21–32.
- Orthous-Daunay, F. R., Quirico, E., Beck, P., Brissaud, O., Dartois, E., Pino, T., and Schmitt, B. 2013. Mid-Infrared Study of the Molecular Structure Variability of Insoluble Organic Matter from Primitive Chondrites. *Icarus* 223: 534–543.
- Osawa, T., Kagi, H., Nakamura, T., and Noguchi, T. 2005. Infrared Spectroscopic Taxonomy for Carbonaceous Chondrites from Speciation of Hydrous Components. *Meteoritics & Planetary Science* 40: 71–86.
- Pilorget, C., Okada, T., Hamm, V., Brunetto, R., Yada, T., Loizeau, D., Riu, L., et al. 2022. First Compositional Analysis of Ryugu Samples by the MicrOmega Hyperspectral Microscope. *Nature Astronomy* 6: 221–25.
- Poch, O., Istiqomah, I., Quirico, E., Beck, P., Schmitt, B., Theulé, P., Faure, A., et al. 2020. Ammonium Salts Are a Reservoir of Nitrogen on a Cometary Nucleus and Possibly on some Asteroids. *Science* 367: eaaw7462.
- Quirico, E., Bonal, L., Beck, P., Alexander, C. M. O'D., Yabuta, H., Nakamura, T., Nakato, A., et al. 2018. Prevalence and Nature of Heating Processes in CM and C2-Ungrouped Chondrites as Revealed by Insoluble Organic Matter. *Geochimica et Cosmochimica Acta* 241: 17–37.
- Quirico, E., Bonal, L., Kebukawa, Y., Amano, K., Yabuta, H., Phan, V. T. H., Beck, P., et al. Compositional Heterogeneity of Insoluble Organic Matter Extracted from Asteroid Ryugu Samples. *Meteoritics and Planetary Science*. Under review.
- Quirico, E., Orthous-Daunay, F.-R., Beck, P., Bonal, L., Brunetto, R., Dartois, E., Pino, T., et al. 2014. Origin of Insoluble Organic Matter in Type 1 and 2 Chondrites: New Clues, New Questions. *Geochimica et Cosmochimica Acta* 136: 80–99.

- Sandford, S. A., Aléon, J., Alexander, C. M. O'D., Araki, T., Bajt, S. A., Baratta, G. A., Borg, J., et al. 2006. Organics Captured from Comet 81P/Wild 2 by the Stardust Spacecraft. *Science* 314: 1720–24.
- Sandford, S. A., Bajt, S., Clemett, S. J., Cody, G. D., Cooper, G., DeGregorio, B. T., De, V. E. R. A. V., et al. 2010. Assessment and Control of Organic and Other Contaminants Associated with the Stardust Sample Return from Comet 81P/Wild 2. *Meteoritics & Planetary Science* 45: 406–433.
- Sawada, H., Okazaki, R., Tachibana, S., Sakamoto, K., Takano, Y., Okamoto, C., Yano, H., et al. 2017. Hayabusa2 Sampler: Collection of Asteroidal Surface Material. *Space Science Reviews* 208: 81–106.
- Tachibana, S., Sawada, H., Okazaki, R., Takano, Y., Sakamoto, K., Miura, Y. N., Okamoto, C., et al. 2022. Pebbles and Sand on Asteroid (162173) Ryugu: In Situ Observation and Particles Returned to Earth. *Science* 375: 1011–16.
- Takano, Y., Yamada, K., Okamoto, C., Sawada, H., Okazaki, R., Sakamoto, K., Kebukawa, Y., et al. 2020. Chemical Assessment of the Explosive Chamber in the Projector System of Hayabusa2 for Asteroid Sampling. *Earth, Planets and Space* 72: 97.
- Uesugi, M., Naraoka, H., Ito, M., Yabuta, H., Kitajima, F., Takano, Y., Mita, H., et al. 2014. Sequential Analysis of Carbonaceous Materials in Hayabusa-Returned Samples for the Determination of their Origin. *Earth, Planets and Space* 66: 102.
- Velbel, M. A., and Zolensky, M. E. 2021. Thermal Metamorphism of CM Chondrites: A Dehydroxylation-Based Peak-Temperature Thermometer and Implications for Sample Return from Asteroids Ryugu and Bennu. *Meteoritics & Planetary Science* 56: 546–585.
- Viennet, J. C., Roskosz, M., Nakamura, T., Beck, P., Baptiste, B., Lavina, B., Alp, E. E., et al. 2023. Interaction Between Clay Minerals and Organics in Asteroid Ryugu. *Geochemical Perspectives Letters* 25: 8–12.
- Yabuta, H., Cody, G. D., Engrand, C., Kebukawa, Y., De Gregorio, B., Bonal, L., Remusat, L., et al. 2023. Macromolecular Organic Matter in Samples of the Asteroid (162173) Ryugu. *Science* 379: eabn 9057.
- Yada, T., Abe, M., Okada, T., Nakato, A., Yogata, K., Miyazaki, A., Hatakeda, K., et al. 2022. Preliminary Analysis of the Hayabusa2 Samples Returned from C-Type Asteroid Ryugu. *Nature Astronomy* 6: 214–220.
- Yada, T., Fujimura, A., Abe, M., Nakamura, T., Noguchi, T., Okazaki, R., Nagao, K., et al. 2014. Hayabusa-Returned Sample Curation in the Planetary Material Sample Curation Facility of JAXA. *Meteoritics & Planetary Science* 49: 135–153.
- Yokoyama, T., Nagashima, K., Nakai, I., Young, E. D., Abe, Y., Aléon, J., Alexander, C. M. O'D., et al. 2023. Samples Returned from the Asteroid Ryugu are Similar to Ivuna-Type Carbonaceous Meteorites. *Science* 379: eabn 7850.

SUPPORTING INFORMATION

Additional supporting information may be found in the online version of this article.

Data S1. Supplementary figures of baseline-correction methods, all optical images and spectra, and table of infrared peak height ratios.